PROCEEDINGS
SPIE—The International Society for Optical Engineering

# Scatter from Optical Components

**John C. Stover**
*Chair/Editor*

**8–10 August 1989**
**San Diego, California**

*Sponsored by*
SPIE—The International Society for Optical Engineering

*Cooperating Organizations*
Applied Optics Laboratory/New Mexico State University
Center for Applied Optics/University of Alabama in Huntsville
Center for Applied Optics Studies/Rose-Hulman Institute of Technology
Center for Electro-Optics/University of Dayton
Center for Excellence in Optical Data Processing/Carnegie Mellon University
Jet Propulsion Laboratory/California Institute of Technology
Optical Sciences Center/University of Arizona
Optoelectronic Computing Systems Center/University of Colorado, Colorado State University

*Published by*
**SPIE—The International Society for Optical Engineering**
**P.O. Box 10, Bellingham, Washington 98227-0010 USA**
Telephone 206/676-3290 (Pacific Time) • Telex 46-7053

SPIE P PROCEEDINGS SERIES

**Volume 1165**

# MEASUREMENT OF LIGHT-BAFFLE ATTENUATION BY A GATING TECHNIQUE

Silvano Donati
Dipartimento di Elettronica
Università di Pavia, 27100 Pavia (Italy)

## 1. INTRODUCTION

High-performance baffles are required in the operation of space sensors mounted aboard a satellite to track stars for attitude control or to identify the sky region aimed by a paralleled X-ray telescope. For example, on a typical X-ray observation mission, the star sensor shall identify stars in a 8 deg by 8 deg field of view down to the 6th magnitude, even when very bright sources (as the sun or the earth horizon) are only 10-15 degrees off the field of view. This corresponds to attenuate stray light down to approximately $10^{-9}$, what calls for a very sophisticated design of the optical baffle and also is an unusual requirement for the measurement of attenuation in the test-laboratory to validate the baffle before launch.[1,2].

Indeed, in a normal laboratory environment, it is found that the light diffused by the baffle blades to the laboratory walls and from here rediffused back into the baffle field of view usually limits the measurable attenuation to $\approx 10^{-6}$.With a careful shielding from this stray contribution, one can reach measurement sensitivities in the range $10^{-8}$-$10^{-9}$ as limited by air-scattering effects in the laboratory, which then require a tight control of contaminants[1-3].

In this paper, we present a new method to perform the attenuation measurement on light-baffles without the disturbance of wall diffusion. The method is based on the use of a fast-pulsed light source, a cavity-dumped Q-switched Nd laser, operating in connection with a fast photomultiplier, so that only light coming directly into the baffle is accepted while light coming with a delay from the walls is gated off (for a few meters distance this delay is some nanoseconds). Secondly, we analyze in detail theoretically the contributions to stray light in a baffle and show how, by means of a two step procedure involving the separate measurements of the light baffle attenuation and of the objective lens scattering, one can evaluate the system attenuation down to $10^{-11}$. In contrast, in a direct measurement with gating the limit of sensitivity in attenuation is about $10^{-9}$.

## 2. THEORY OF SYSTEM ATTENUATION

Let us schematize as in Fig.1 the optical system of a star sensor as the combination af a baffle and an objective lens. Here, the field of view (fov) $\alpha_b$ of the baffle is assumed slightly larger than the fov $\alpha$ of the objective so that, as it is necessary to achieve a high attenuation, the baffle blades are not seen in the image field defined by the aperture of the photodetector.

As a definition of *attenuation*, one can assume different ratios of output-to-input radiant quantities. For example, one can take as in Ref.1 the *radiant power attenuation* of the baffle $A_{pb}$ as:

$$A_{pb} = P_{ob}/P_{ib} \tag{1}$$

and similarly the radiant power attenuation of the objective lens as:

$$A_{pl} = P_{ol}/P_{il} \tag{2}$$

where P's are the radiant powers (Watt) and the indexes indicate: i- the input, o- the output, b- the baffle, l- the lens (Fig.1). From (1) and (2) the total attenuation follows as $A = A_{pl} \cdot A_{pb}$, but the exact partition between $A_{pl}$ and $A_{pb}$ depends on the angular distribution of power at the baffle output plane. In addition, $A_{pb}$ is of little significance if the measurement of $P_{ob}$ is performed without excluding the large contribution coming from the blades. To have the attenuation as the product of two independent quantities, each separately measurable and specific of the baffle and of the objective respectively, it is better to define the baffle attenuation $A_b$ as:

$$A_b = [\text{ output radiance / input irradiance }] = R_{ob} / E_{ib} \tag{4}$$

and the objective lens attenuation as:

$$A_l = [\text{ output irradiance / input radiance }] = E_{ol} / R_{il} \tag{5}$$

so that their product, being $R_{ob} = R_{il}$ (Fig.1), follows as:

$$A = A_b \cdot A_l \tag{6}$$

Let us now compute the irradiance $E_{oI}$ at the output image field when the optical system is aimed at an incidence angle $\theta$ respect to a stray bright source giving an irradiance $E_i$ onto the input pupil of the baffle. Firstly, from the definition of $A_b$ and using the cosine law we have:

$$R_{ob} = A_b\, E_i \cos\theta \tag{7}$$

where in general $R_{ob}$ will depend on the coordinates x,y of the baffle output plane as well as on the angles $\eta,\psi$ of the ray direction. However, the dependence on x,y is found experimentally to be modest, and for sake of simplicity we will ignore it in the following (if not, one should simply modify all subsequent expressions with an integration on x,y). Secondly, we can write the radiance R produced by scattering in the objective lens as the integral of the contribution $R_{ob}$ at the angle $\xi$ (Fig.2) weighted by the lens scattering function $F_s$(see below):

$$R(\psi) = \int_\Omega R_{ob}(\xi)\, F_s(\zeta)\, d\Omega = \int_0^{\pi/2} R_{ob}(\xi)\, F_s(\zeta)\, 2\pi \sin\xi\, d\xi, \tag{8}$$

where, from spherical trigonometry, $\zeta$ is found as:

$$\cos\zeta = \cos\psi\cos\xi + \sin\psi\sin\xi\cos\phi \tag{9}$$

and $\phi$ is the azimuth angle associated with $\xi$ ($\phi = 0\text{-}2\pi$ along the rotation of the vector i out of the plane of Fig.2). Finally, we have for the irradiance $E_{oI}$ on the focal plane:

$$E_{oI} = (dP/dS) = (1/dS) \int_\Sigma R(\psi)\, d\Sigma\, d\Omega \tag{10}$$

Eqs.(8-10) are difficult to treat in closed form, and to get an insight let us take as first-order approximations: (i), a truncated Lambertian distribution in $\eta,\psi$ for the radiance $R_{ob}$, i.e., $R_{ob}(\xi) = R_{ob}\cos\xi$ for $\xi \geq \alpha_b$, and $R_{ob}(\xi) = 0$ for $\xi < \alpha_b$ (see Fig.3), and (ii), an objective lens with small aperture $\alpha_o$ so that $\psi = 0$ and $\xi = \zeta$ in Eq.(9). Then Eq.(8) becomes:

$$R(\psi) = R_{ob} \left\{ 2\pi \int_{\alpha_o}^{\pi/2} \cos\xi\, \sin\xi\, F_s(\xi)\, d\xi \right\} = R_{ob} \cdot F \tag{11}$$

i.e., $R(\psi)$ is independent from $\psi$ and the scattering is summarized by the constant factor $F$. By using the expressions for $d\Sigma$, $d\Omega$ calculated from Fig.2 as:
$d\Sigma = 2\pi F \tan\psi\, (F\, d\psi / \cos\psi)$ and $d\Omega = dS\, \cos\psi / (F^2/\cos^2\psi)$,
F being the objective focal length, we get for the irradiance on the image field [Eq.(10)]:

$$E_{oI} = \int_0^{\alpha_o} R_{ob} F\, 2\pi \cos\psi\, \sin\psi\, d\psi = R_{ob} F\, \pi \sin^2\alpha_o \tag{12}$$

which is an expected result in view of the dependence from the numerical aperture $\sin\alpha_o$ of the objective lens. At any rate, note that the factor $F$ defined in brackets in Eq.(11) summarizes the scattering effect of the objective lens, and for small $\alpha_o$ it coincides with the paraxial scattering factor usually quoted as a scattering specification for an objective lens. Going back to Eqs.(4-6) and comparing to Eqs.(7, 10,11), the total attenuation is found as:

$$A = A_b\, F\, \pi \sin^2\alpha_o\,, \tag{13}$$

where the second term shows that the lens attenuation $A_l$ is given in general by:

$$A_l = F\, \pi \sin^2\alpha_o. \tag{14}$$

This expression can also be written in general, when the above assumptions of truncated Lambertian distribution and small aperture do not hold, provided $F$ is evaluated exactly (e.g. by numerical integration) from Eqs.(8-11) using the radiance distribution $R_{ob}(\xi)$ of which $R_{ob}$ is the equivalent-Lambertian average.
For sake of clarity, let us discuss the lens scattering function $F_s$ used in Eq.(8), which is defined as:

$$F_s(\zeta) = (1/K)\ dP(\zeta) / P\ d\Omega, \quad (15)$$

where $d\Omega$ is the solid angle at $\zeta$ where the power $dP(\zeta)$ is scattered, and K is the total attenuation factor by scattering or normalizing factor, $\int dP / P = K$. An usually employed expression for $F_s(\zeta)$, which fits fairly well the experimental data for lenses in the range $\zeta$ = 1 - 10 deg is [4]: $F_s(\zeta) = c\ (\sin \zeta)^{-n}$, where n = 1 - 1.5 and the constant c is from $10^{-2}$ to $10^{-4}$ according to lens cleaniness. Using the definition [Eq.(12)] of $F$ and assuming n=1 one obtains from the normalization condition:

$$F = (2/\pi)\ (1 - \sin \alpha_o)\ K. \quad (16)$$

The factor $F$ is the usually quoted specification given for a lens, measured as the ratio $F = E_{sc} / E_i$ of scattered irradiance $E_{sc}$ collected in the image plane when the object is a black spot divided by the irradiance $E_i$ of the uniform bright field surrounding the black spot.

## 3. ANALYSIS OF STRAY LIGHT IN LABORATORY MEASUREMENTS

There are several distinct sources of stray rays which contribute to limit the performance of a baffle, either in the space operation or in the laboratory environment. We will now analyze these sources with the aim of: (i) finding the maximum allowable values of the relevant quantities in a laboratory measurement; (ii) comparing the effectiveness of the *direct* methods (one measurement on the baffle and objective assembly) versus the *indirect* methods based on two separate measurements on baffle and objective and the calculation of the total attenuation through Eq.(6).

As shown in Fig.4, the breakdown of stray light contributions is the following:

a) rays scattered (or reflected) by the baffle blades and transmitted through the lens [fall outside the field of view]

b) rays scattered (or reflected) by the baffle blades and scattered by the lens [fall inside the field of view]

c) rays scattered from blades and baffle structure to the laboratory walls, and from here scattered back through the lens [fall inside the field of view]

c') (not shown in Fig.4) as in c) but scattered by the lens [a minor contribution, generally outside the field of view]

d) rays scattered by the air within the volume V (Fig.4) [fall inside the field of view]

d') (not shown in Fig.4) as in d) but scattered by the lens [a minor contribution, generally outside the field of view].

Contributions a) and b) are those only affecting the space operation of the system, while c) and d) are the most serious added terms affecting the laboratory performance. To quantify these terms, let us consider three irradiances which can be measured in the system, namely: $E_{ob}$, the irradiance at the baffle output, as in Fig.1; $E_{ol,fov}$, the irradiance at the focal plane inside the field of view, and $E_{ol,ext}$, the irradiance at the focal plane falling outside the field of view. Then, if $E_{ib}$ is the input irradiance we can write the terms found in a laboratory measurement as:

$$E_{ob} = A_b\ \pi\ E_{ib} + E_{scatt} + E_{wall} \quad (17)$$

$$E_{ol,fov} = A_b\ A_l\ E_{ib} + E_{scatt}\ \sin^2 \alpha_o / \sin^2 \alpha + E_{wall}\ \sin^2 \alpha_o \quad (18)$$

$$E_{ol,ext} = A_b\ \pi\ \sin^2 \alpha_o\ E_{ib} + E_{scatt}\ \sin^2 \alpha_o / \sin^2 \alpha\ F + E_{wall}\ \sin^2 \alpha_o\ F \quad (19)$$

where $\alpha$, $\alpha_o$, $\alpha_b$, $F$ are defined above and $E_{scatt}$, $E_{wall}$ are the irradiances at the baffle output pupil due to scattering and of the wall illuminated by the baffle blades, which are calculated (at first order) as:

$$E_{scatt} = \sigma_{air}\ V / H^2\ E_{ib} \quad (20)$$

$$E_{wall} = \rho_{baf}\ \rho_{wall}\ [d^2 / (D+H)^2]\ E_{ib} \quad (21)$$

where $\sigma_{air} = d^2P / P\ dz\ d\Omega$ is the air differential scattering function, $\rho_{baf}$ and $\rho_{wall}$ are the albedos of the baffle blades and of the wall respectively, V is the scattering volume (Fig.4), D is the wall distance and H, d are height and output diameter of the baffle.

Now, let us take representative values of the above quantities to illustrate the relative importance of air scattering and wall diffusion in three different possible measurements. For a baffle with H=50 cm, d=6 cm, $\rho_{baf}$ =0.05, $\alpha_b$ =4 deg operating with an objective lens of aperture $\sin^2 \alpha_o$=0.5 and scattering factor $F$ =0.03, under measurement in a laboratory room with a front wall at a distance D=2 m with $\rho_{wall}$ =0.1, and with $\sigma_{air}$ =1.5· $10^{-9}$ $cm^{-1}$ $sr^{-1}$ (typical of a class 100 ambient), we have for an incidence at $\theta$=45 deg from Eqs.(17-21):

$$E_{ob} / E_{ib} = A_b\ \pi + 2.73 \cdot 10^{-9} + 0.72 \cdot 10^{-6} \quad (22)$$

which shows that the wall scattering dominates in a measurement simply done by integrating the collected power at the baffle output. To tackle this effect, one should increase the distance D or reduce the wall albedo $\rho_{wall}$. At any rate, it is difficult to increase substantially the sensitivity beyond $10^{-7}$, as discussed in Refs.1,2. By the use of a range-gating technique capable of eliminating the wall-diffused contribution, the limit of a direct measurement on $E_{ob}$ becomes that of air scattering, i.e. around $10^{-9}$, provided a good conditioning of air cleaniness in the region illuminated by the light beam and viewed by the baffle (Fig.4) is ensured.
With the same numerical values, the irradiance falling in the fov at the focal plane is:

$$E_{ol,fov} / E_{ib} = A_b A_l + 2.76 \cdot 10^{-7} + 7.3 \cdot 10^{-5} \quad (23)$$

e.g., the useful signal given by the first term is decreased (by $A_l$) and the second and third unwanted terms are increased. While there is obviously no advantage in performing a direct measurement in the fov at the focal plane, this scheme may be useful to evaluate the amount of disturbing contribution (mainly the wall diffusion in continuos-wave and the air scattering in gated operation). Lastly, the irradiance falling outside the fov at the focal plane is:

$$E_{ol,ext} / E_{ib} = A_b \cdot \pi \sin^2 \alpha_o + 2.76 \cdot 10^{-7} F + 7.3 \cdot 10^{-5} F \quad (24)$$

for which, assuming $F$ =0.03 as it is representative of a 9-element space-sensor objective with $\sin^2 \alpha_o$ =0.5 we have:

$$E_{ol,ext} / E_{ib} = A_b \cdot 1.57 + 8.29 \cdot 10^{-9} + 2.2 \cdot 10^{-6} \quad (24')$$

i.e. a value slightly worse than that pertaining to the direct measurement at the baffle output. However, if we employ for this measurement a separate, single element lens instead of the actual objective, we may work with $F$ =0.003 and $\sin \alpha_o$ =0.25 thus obtaining:

$$E_{ol,ext} / E_{ib} = A_b \cdot 0.39 + 2.06 \cdot 10^{-10} + 5.5 \cdot 10^{-8} \quad (25)$$

In conclusion, let us compare the different limits of sensitivity achieved in attenuation measurements by letting $A_b$ equal to the other added terms in Eqs.(17-19) or numerically using Eqs.(22-25). In a direct, no-gating measurement at the baffle output, the limit is [Eq.(22)] $A_b = 0.72/\pi \; 10^{-6} = 2.3 \; 10^{-7}$, while with gating it is $A_b = 2.73/\pi \; 10^{-9} = 0.87 \; 10^{-9}$. If we move at the focal plane of a clean lens, outside the fov, we get [Eq.(25)] $A_b = 1.4 \; 10^{-7}$ (no gating) and $0.53 \; 10^{-9}$ (gating) respectively. With the separate measurement of the objective scattering factor $F$ and using Eq.(14) to evaluate $A_l$, we get as limit of measurable attenuation of the baffle/objective system the typical values $A = 7 \; 10^{-9}$ (no gating) and $A = 2.6 \; 10^{-11}$ (gating). This sensitivity can be furtherly improved by subtracting the air scattering contribution measured independently in the fov at the focal plane with gating [Eq.(23)].

## 4. EXPERIMENTAL

An overview of the installation used in the measurements is shown in Fig.5. The optical source is a Nd-YAG laser operating in Q-switching and cavity dumping mode, with second-harmonic genaration, and it supplies short (4 ns duration) pulses at $\lambda$ = 0.53 μm. The source is located in a separate room, so as to minimize both stray light level and electromagnetic interference due to the fast switching of electronic drives. The beam is sent into the measurement room after a delay (again to reduce EMI). Here, the beam is first sensed by a beamsplitter and a photomultiplier which gives the reference signal of input power and also the trigger to the electronics. Then the beam is directed, properly screened with black panels, to the projection optics which widens it so as to fill the baffle input pupil. The baffle is mounted on a rotatable platform to scan the incidence angle θ from 0 to nearly 90 deg. As the baffle is rotated, the projection diaphragm is also rotated keeping it parallel to the baffe, so that the projected spot always matches the input baffle pupil without over- or underfilling. At the baffle output, a photomultiplier equipped with a stack of neutral density filters measures the incoming flux, which gives directly the irradiance distribution versus θ. The reference channel allows to correct the measurement against the power fluctuations from pulse to pulse (typ. ±10%). In addition, by inserting a lens at the baffle output and sampling the focal plane with a stop, the angular distribution of the irradiance can be measured. The wall diffused contribution is easily gated off since there is an adequate delay (≈10 ns) respect to the direct pulse. A laminar flow air-condi tioning cap is used to keep clean the air in the scattering volume in front of the baffle, down to $\approx 10^{-9}$ level.

### 4.1 The laser source

As shown in Fig.6, the laser source is built around two Nd-YAG rods pumped by linear flashlamps, the first used in a Q-switched oscillator with pulse slicer to provide a short 1.06 μm pulse, the other serving as a two-pass amplifier to boost the pulse energy up to 25 mJ; a second-harmonic crystal finally converts the emission in the visible at $\lambda$ = 0.53

μm. The flashlamps are driven in synchronism with a proper delay for master-slave operation. In the optical cavity of the oscillator (mirrors M1-M2), the Pockel cell and quarter-wave plate are the usual electrooptic switch which is required for a Q-switched mode. To shorten the pulse duration of this mode, which is typically 20 ns at half maximum, a cavity dumping section is added (Glan cube and Pockel cell slicer). When power in the cavity builds up to a proper threshold value, a fast photodiode triggers a high-voltage 2-ns risetime pulser driving the Pockel slicer, and the polarization becomes rotated by 90 deg. Light coming back to the Glan cube is therefore deflected outside the cavity down to mirror M3. Since it takes a cavity roundtrip time to fully dump the cavity, a duration of the emitted pulse $2L/c = 5$ ns is obtained, with a typical pulse energy ≈0.2 mJ. With the folded path defined by four mirrors M (Fig.6), the beam size is expanded to match the amplifier rod diameter and is two-pass amplified up to 25 mJ. At this level, the efficiency of the SHG crystal is fairly high and 15 mJ energy per pulse is delivered at the output. Moreover, due to the nonlinear SH process, the pulse width is shortened to 4 ns (full width half maximum).

4.2 Transmitting optics

The laser baem is sent into the measurement room after a folded propagation (Fig.5) on a 7.5m path to add a 50 ns optical dalay, useful to avoid EMI from the Pockel cells to the photomultipliers. The ≈1 mr divergence of the beam allows easily to block by screens and pinholes the spurious spots due to reflections and diffractions. A beam-steering optics is used for height matching and includes an interference filter to cut out the residual slow pedestal at 1.06 μm leaking through the SHG crystal. In front of the reference photomultiplier, located at the measurement-room entrance, a glass plate oriented close to Brewster angle is used to pick up a small percentage of the beam power. The projection optics is made by a negative lens and an aperture stop mounted on a rotatable platform so that: (i) only the central part of the gaussian beam is selected to ensure a good uniformity of illumination, (ii) the matching of beam to baffle input pupil is ensured at all incidence angles.

4.3 Detectors

For both measurement and reference channels, two XP 2230B (Philips) photomultipliers were used. With a 50 mA/W radiant sensitivity at $\lambda = 0.53$ μm and a $2 \cdot 10^7$ gain at 2500V supply voltage, the single electron response was readily measurable (1 mA peak) on a fast oscilloscope (Tektronix 7904). With a so-called type-B' dynode voltage-divider, the single-electron-response risetime is 1.6 ns and the half-maximum duration is 2.7 ns, i.e. is adequate for the 4 ns pulses, while the linearity is better than 2% up to 70 mA of peak current, i.e. allowing for a satisfactory dynamic range (a factor >70). In a single measurement, the rms error due to the photoelectron and multiplier statistics was measured to be 10% on peak amplitude, and 3% on total collected charge (at 30 mA peak current). In front of the photocathode, a stack of neutral density filters (96 Wratten) were used to coarsely adjust the input power level. Routinely, the coarse attenuation was varied from 1 to 9 O.D. (or $10^{-1}$ to $10^{-9}$) as the incidence angle varied from $\theta$=10 to 70 deg. With the available laser power collected at $\theta$=0 deg, the barely measurable attenuation (or dynamic range of the system) was about 12.7 O.D.

4.4 Baffle

Baffles with dimensions up to 1.5m length, 70 cm diameter can be accomodated in the setup. The measurements reported below were performed on a maquette (or engineering model) of a star-sensor baffle, a two-stage unit with 63cm length, 200/60mm input/output pupils, and $\alpha_b = \pm 9$ deg (first stage), $\alpha_b = \pm 3$ deg (second stage). The baffle is intended to allow the detection of +6 m stars when the sun (-27 m) is at ≥40 deg incidence angle, which amounts to require an attenuation $A \approx 10^{-8}$.

## 5. MEASUREMENTS

Typical waveforms of reference and measurement signals as seen at the oscilloscope at different incidence angles $\theta$ are reported in Fig.7. At increasing incidence angle $\theta$, the measurement signal strongly decreases and, by reducing the coarse attenuation to recover it in amplitude, the spurious pulses due to wall-diffusion become increasingly evident as well as the weaker air-scattered contribution.

Both direct and indirect (focal plane) measurements were performed. The result of a direct measurement of baffle attenuation $A_b$ versus $\theta$ is shown in Fig.8 (full line curve). Here, respect to the $\theta$=0 deg signal level, the sensitivity limit of the system was $0.2\ 10^{-11}$. The air-scattering limit was measured letting the illuminating beam to pass in front of the baffle without impinging on it, and its trend versus $\theta$ was extrapolated according to the scattering volume $V=V(\theta)$, as also reported in Fig.8 (dashed area). A substantial variation from day to day of the air-scattering level was observed, which has been ascribed to the varying efficiency of air conditioning cap over the baffle.

Indirect measurements were carried out with a single-element lens (D=60mm, F=150mm) and scanning the focal plane with the photomultiplier. In Fig.9 the reletive irradiance measurement is reported as a function of the exit angle $\psi$ and with the incidence angle $\theta$ as a parameter. Besides the general decreasing trend with increasing $\theta$, sharp peaks are noted outside the field of view defined by the baffle angle $\alpha_b$. The decrease for $\psi$ >10 deg is due to the two-stage structure, in which the first stage blades becomes shadowed by the second stage blades. The peak at $\psi$ =-10 deg, $\theta$=+10 deg, is due to the direct illumination of the bottom second-stage blades. Using the data of Fig.9 and Eqs.(17-21), one can compute the result reported in Fig.8 (broken line) as the baffle/objective total irradiance attenuation A of the optical system (an objective with $F$=0.03 and a numerical aperture $\sin^2 \alpha_0$ =0.5 has been assumed in the calculation).

As a concluding remark, the gating technique proposed in this work has been demonstrated capable of measuring attenuations of light baffles down to $10^{-9}$ in direct measurements and to $10^{-11}$ in indirect measurements. Accuracy and repeatibility are good and the experimental arrangement is amenable to fully automated data acquisition and processing through computer control.

## 6. ACKNOWLEDGEMENTS

The author carried out this work at CISE-Tecnologie Innovative, Milano (Italy), under contract with the Italian Space Agency (ASI) of the National Research Council (CNR), and thanks CISE and ASI for the permission to publish this paper. He also thanks dr. Malvicini for the laser source and Mr.Daino for the skillful work.

## 7. REFERENCES

1. C. Leinert, D. Kluppelberg, "Stray Light Suppression in Optical Space Experiment", *Applied Optics*, vol.13, pp.556-561, 1974.

2. J.C. Kemp, C.L. Wyatt, "Terrestrial Measurements of the Performances of High-Rejection Optical Baffling System", *Proc. SPIE Conf. No.91*, pp.85-92, 1976.

3. F.W. Schenkel, "A Self Deployable High Attenuation Light Shade for Spaceborn Astronomical Sensors", *Journal of Britain Interplanetary Soc.*, vol.26, pp.589-594, 1973.

4. G.R. Hostetter, D.L. Patz, H.A. Hill, C.A. Zanoni, "Measurement of Scattered Light from Mirrors and Lenses", *Applied Optics*, vol.7, pp.1983-1988, 1968.

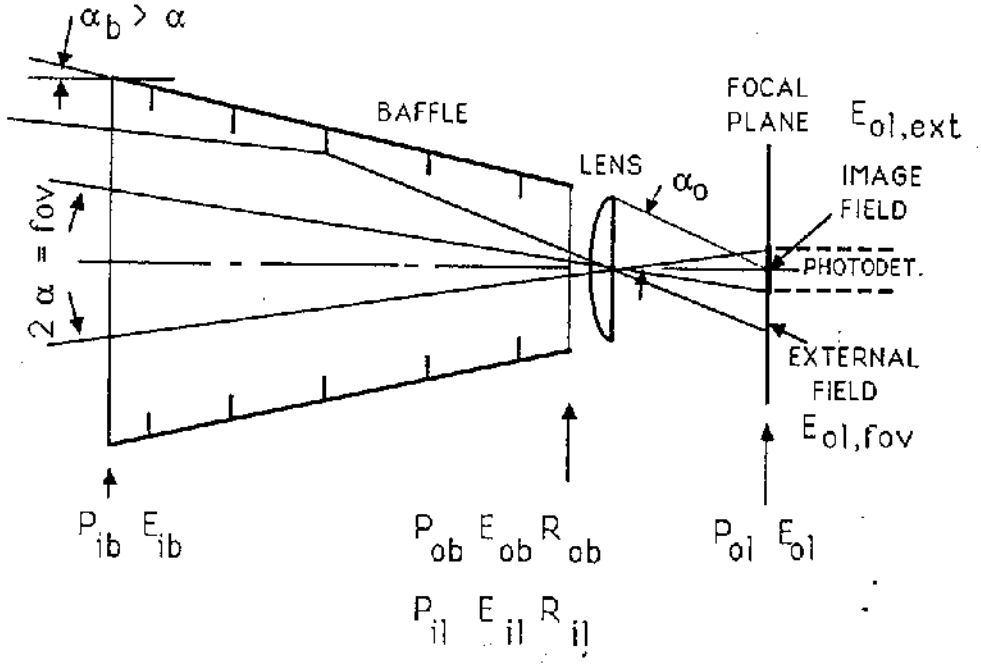


Fig. I Model of the baffle and objective optical system.

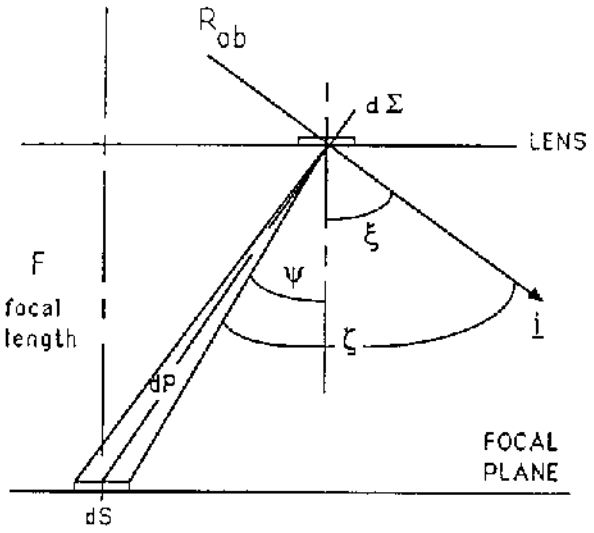


Fig.2 Geometry of lens scattering

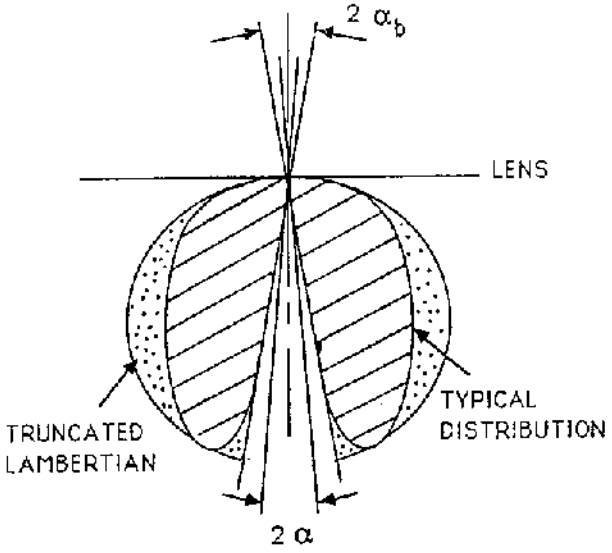


Fig.3 Scattering distribution

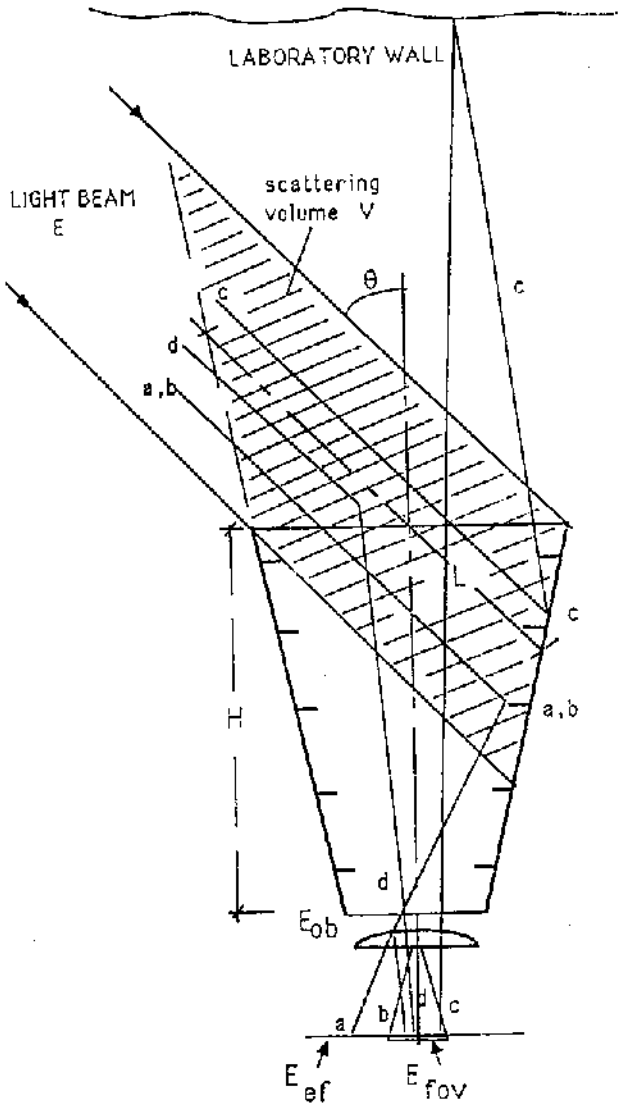


Fig.4 Breakdown of stray light contributions

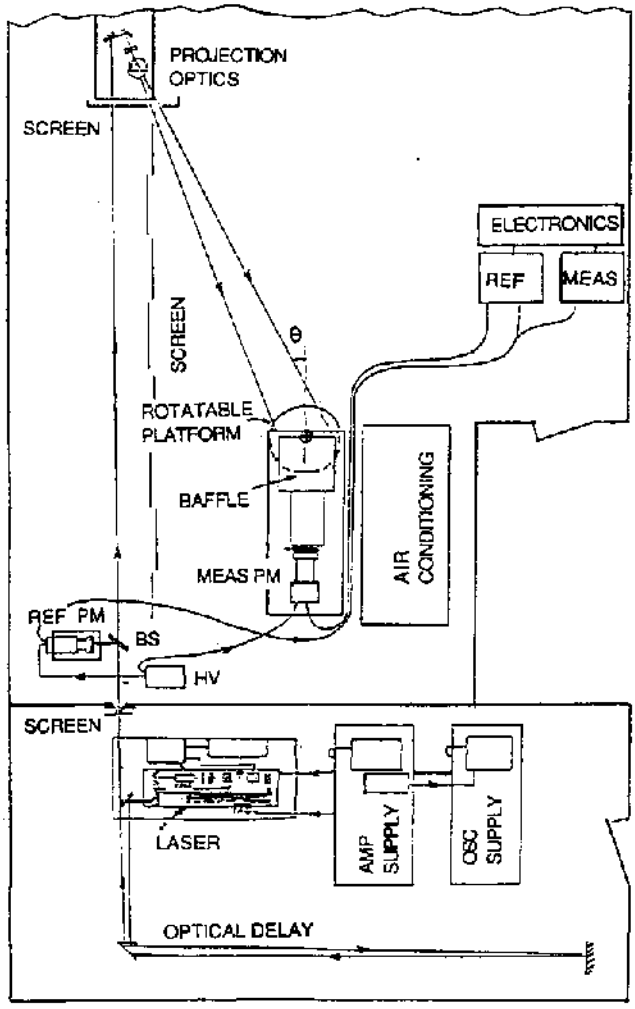


Fig.5 Layout of measurement installation

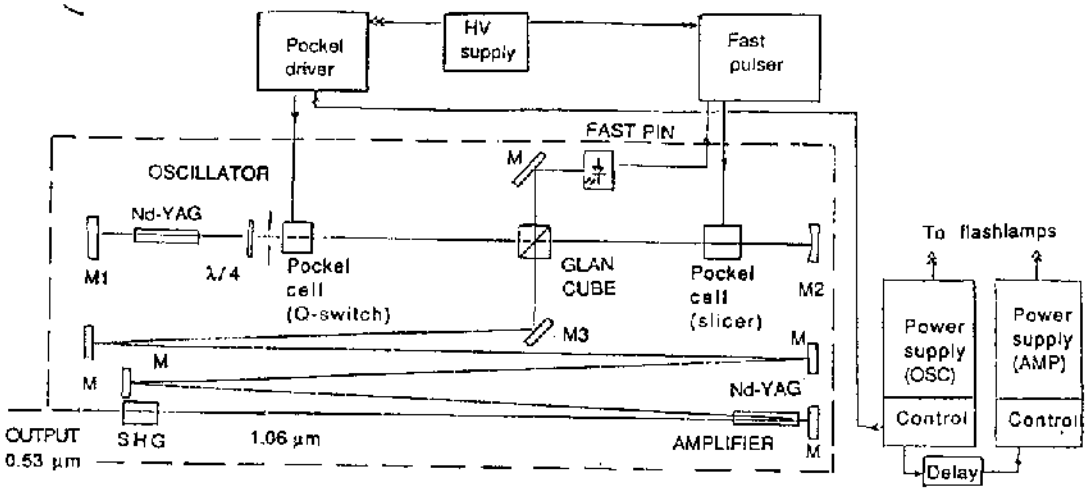


Fig.6 Laser source schematic

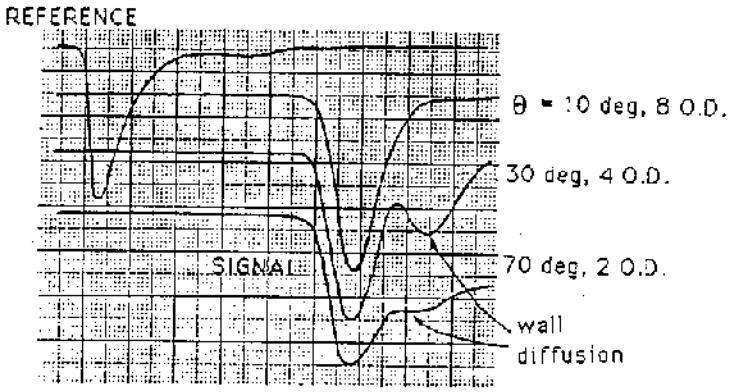


Fig.7 Typical reference and signal waveforms at different inclination angles θ and corresponding O.D. attenuations. Time scale: 5 ns per major division

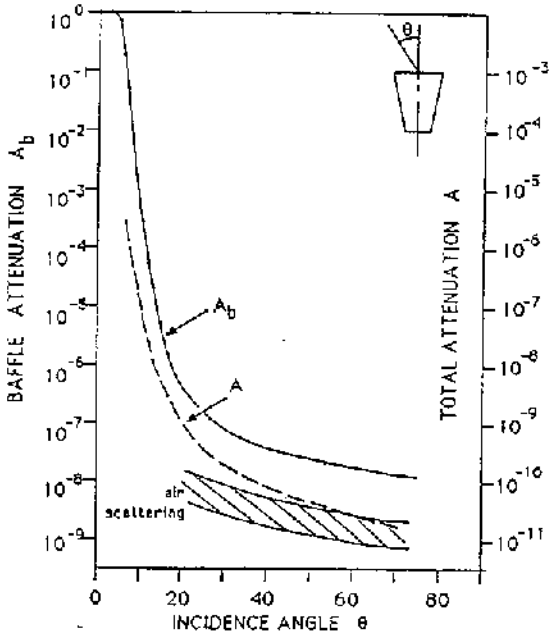


Fig.8 Measured irradiance attenuation $A_b$ (full line) and computed total attenuation A

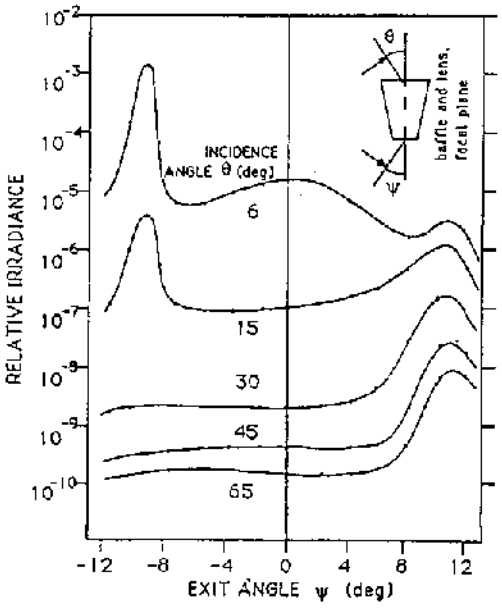


Fig.9 Measured relative irradiance in the focal plane